Aharonov-Bohm detection of two-dimensional magnetostatic cloaks

Constantinos A. Valagiannopoulos
Department of Physics, School of Science and Technology, Nazarbayev University, 53 Qabanbay Batyr Avenue, Astana KZ-010000, Kazakhstan

Amir Nader Askarpour
Department of Electrical Engineering, Amirkabir University of Technology, 424 Hafez Avenue, Tehran 15875-4413, Iran

Andrea Alù
Department of Electrical Engineering, University of Texas at Austin, 1616 Guadalupe Street, Austin, Texas 78701, USA

(Received 29 September 2015; revised manuscript received 16 November 2015; published 10 December 2015)

Two-dimensional magnetostatic cloaks, even when perfectly designed to mitigate the magnetic field disturbance of a scatterer, may be still detectable with Aharonov-Bohm (AB) measurements, and therefore may affect quantum interactions and experiments with elongated objects. We explore a multilayered cylindrical cloak whose permeability profile is tailored to nullify the magnetic-flux perturbation of the system, neutralizing its effect on AB measurements, and simultaneously optimally suppress the overall scattering. In this way, our improved magnetostatic cloak combines substantial mitigation of the magnetostatic scattering response with zero detectability by AB experiments.

DOI: 10.1103/PhysRevB.92.224414 PACS number(s): 41.20.Gz, 03.65.Ta, 94.05.Pt, 85.25.Dq

I. INTRODUCTION

Making an electromagnetic object of arbitrary shape and texture invisible to certain portions of the frequency spectrum is one of the most intriguing possibilities offered by metamaterials. Several attempts have been made to achieve substantial mitigation of scattering by passive objects, from the modification of optical ray paths using inhomogeneous and anisotropic cloaks [1] to scattering cancellation by destructive interference using anti-scattering covers [2,3]. For passive cloaking systems, the electrical size of the cloaked object is the fundamental bottleneck to suppress scattering over a broad spectral range [4], as may be expected from simple causality arguments. Quite interestingly, it was recently shown that the overall scattering cross section of an arbitrary passive object, when integrated over all frequencies, becomes larger when cloaked than in the uncloaked scenario [4]. This conclusion stems from the general relation between the static scattering signature of an object and its integrated scattering cross section [5,6]. An intriguing exception to this general limitation of passive cloaks was found in the case of certain classes of magnetostatic superconducting cloaks [7], which may be able not only to suppress the static distortion to the applied field, but also to reduce the overall scattering cross section integrated over all frequencies. This brings attention to magnetostatic superconducting cloaks, which become a particularly important class for the entire field of cloaking and scattering manipulation with metamaterials.

In one attempt [8] to design a magnetic cloak at zero frequency, variable, anisotropic magnetic permeability with both paramagnetic and diamagnetic components was considered. A metamaterial geometry that can be used to tailor the required magnetic response has been presented [9], while another implementation of transformation optics in magnetostatics was pushed forward [10]. Experimental verification of a magnetostatic cloak [11] has been based on the scattering cancellation approach, for which no anisotropic or inhomogeneous media are necessary. An alternative experimental demonstration [12] was reported in the quasistatic regime, and a magnetostatic carpet cloak [13] to hide objects over a superconducting plane is based again on transformation optics.

Interestingly, a vanishing scattering magnetostatic field does not necessarily imply that the cloaked object is undetectable for an observer placed around the object. As observed several decades ago by Aharonov and Bohm [14,15], a nonzero magnetic flux through a closed loop (C) can be detectable even in regions around the loop for which the magnetostatic field is zero. In the original work [14] of Aharonov and Bohm, a completely shielded structure containing axial magnetic currents was detected measuring the phase difference ($\oint_{(C)} \mathbf{A} \cdot d\mathbf{l} \neq 0$) between electron beams traveling around the enclosed region (C), on a path over which no fields were recorded ($\mathbf{B} = \mathbf{0}$). The so-called Aharonov-Bohm (AB) effect, associated with the nonlocalized wave nature of electron beams, still remains a source of surprising and thought-provoking results [16], while many different versions and variations have been formulated [17].

In this study, we explore whether an ideal two-dimensional (2D) magnetostatic cloak, despite having identically zero magnetostatic scattering, may be detected using electron beams, based on an analog of the AB experiment. Since the Aharonov-Bohm effect is at the basis of several sensing schemes [18–20], it is relevant to consider whether the cloaked object would actually perturb a sensing measurement performed in its vicinity, or whether it may be detected with a quantum-sensing scheme. After verifying its detectability, we look for solutions to mitigate it. More specifically, we develop a multilayered, perturbed version of the magnetostatic cloak [11] to suppress the magnetic flux through the object while we simultaneously retain an overall low scattering response. We observe the magnitude of scattering suppression caused by the cloak in the presence of homogeneous background magnetic fields of arbitrary direction, and the variation of

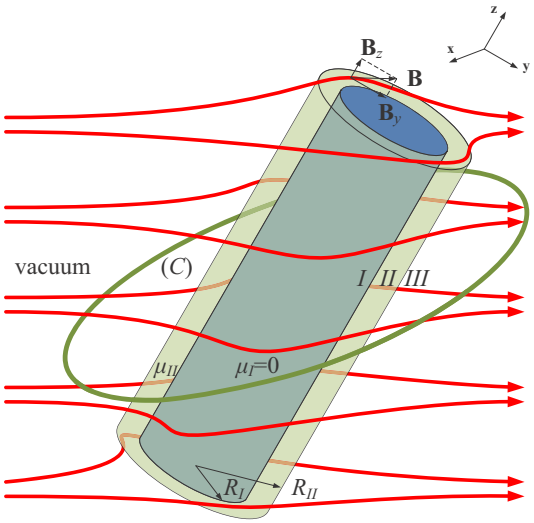

FIG. 1. (Color online) Schematic of the two mechanisms to detect the superconducting ($\mu_{\rm I}=0$) 2D cylindrical volume $\rho<R_{\rm I}$. Due to the presence of a suitable ($\mu_{\rm II}$) cladding ($R_{\rm I}<\rho<R_{\rm II}$), the magnetic field lines (red in figure) "avoid" the internal object and a perfect restoration of the background field $\mathbf{B}_{\rm back}$ is achieved from the other side; therefore $\mathbf{B}_{\rm scat,III}=\mathbf{0}$ into region III ($\rho>R_{\rm II}$). However, the line integral of the magnetic vector potential along a closed loop (C) (green line) is nonzero ($\oint_{(C)}\mathbf{A}_{\rm scat}\cdot d\mathbf{l}\neq 0$) which makes the rod of region I ($\rho<R_{\rm I}$) detectable through AB measurements.

the magnetic flux when the cloaked superconducting object contains inclusions.

II. ANALYTICAL FORMULATION

A. Magnetostatic cloak

The idea of a magnetostatic cloak has been originally proposed in [11] based on the scattering cancellation approach [2]. The presented concept refers to an infinite cylindrical structure with axis parallel to the $\hat{\mathbf{z}}$ axis of the Cartesian coordinate system (x,y,z) [or alternatively the corresponding cylindrical coordinate system (ρ,φ,z)], as sketched in Fig. 1. The cloaked region (region I), of radius $R_{\rm I}$, is circular and filled with a superconducting material ($\mu_{\rm I}=0$) that makes it impenetrable to any background magnetic field $\mathbf{B}_{\rm back}$, enabling the designer to hide any object inside it. Around it, the cylindrical cloak (region II) has relative magnetic permeability $\mu_{\rm II}$ and an external radius $R_{\rm II}>R_{\rm I}$. It is easy to verify that the design rule

$$\mu_{\rm II}=\frac{R_{\rm II}^2+R_{\rm I}^2}{R_{\rm II}^2-R_{\rm I}^2} \tag{1}$$

makes the 2D magnetostatic scattering from the coated structure identically zero $\mathbf{B}_{\rm scat,III}=\mathbf{0}$, i.e., the magnetostatic field all around (region III) the cloaked object is identical to the impressed one. The cloak is actually designed to suppress the scattering originating from the applied magnetostatic field normal to the cylinder axis, since the other polarization (magnetic field parallel to the $\hat{\mathbf{z}}$ axis) does not have any effect on the scattering for a 2D cylinder.

Even under the ideal conditions (1), for which the magnetostatic field distribution all around the object is identical to the incident one, the cloak may be detected performing an AB experiment [14], because, while the scattered fields are identically zero around it, the scattered magnetic vector potential is not. More specifically, the wave function of an electron (charge q) beam traveling in a zero-scattering region involves the line integral of the scattered magnetic vector potential ($\mathbf{A}_{\rm scat}$) over the trajectory (T) of the particle [14]: $\int_{(T)}\mathbf{A}_{\rm scat}\cdot d\mathbf{l}$, which provides a nonzero contribution to the total accumulated phase factor $\exp\left(\frac{jq}{\hbar}\int_{(T)}\mathbf{A}_{\rm scat}\cdot d\mathbf{l}\right)$, even in the case of an ideally cloaked object ($\hbar$ is the reduced Planck constant).

This implies that two identical particles with charge q traveling in the outer zero-field region III would be characterized by different wave functions if the magnetic vector potential $\mathbf{A}_{\rm scat}$ is different along their trajectories, even though the local magnetostatic scattered field is equal to zero. Therefore, the cloaked object, while producing no scattered fields in the background (region III) is, interestingly, detectable by a pair of electron beams, since their measured phase difference will be different if the cloaked object is present or is not, provided that the line integral of $\mathbf{A}_{\rm scat}$ around a closed loop containing the cloaked cylinder is nonzero: $\oint_{(C)}\mathbf{A}_{\rm scat}\cdot d\mathbf{l}\neq 0$. After solving the scalar boundary-value problem, we obtain

$$\oint_{(C)}\mathbf{A}_{\rm scat}\cdot d\mathbf{l}=\int_{(S)}(\nabla\times\mathbf{A}_{\rm scat})\cdot d\mathbf{s}$$
$$=\int_{(S)}\mathbf{B}_{\rm scat}\cdot d\mathbf{s}=\pi(\hat{\mathbf{z}}\cdot\mathbf{B}_{\rm back})R_{\rm I}^2, \tag{2}$$

where we choose the surface (S) in a way that it passes through the cloaked cylinder perpendicular to the $\hat{\mathbf{z}}$ axis. This is allowed because $\mathbf{B}$ is divergence free and deforming (S) does not change the flux that passes through it. Therefore, the integral reduces to an integral over the cross section of the cloaked cylinder, because of the fact that $\mathbf{B}_{\rm scat}=\mathbf{B}-\mathbf{B}_{\rm back}=\mu_0\mu_r\mathbf{H}-\mu_0\mathbf{H}_{\rm back}$ (μ_r is the local relative magnetic permeability of each region) is identically zero outside the cloaked cylinder by definition. Furthermore, the quantity $\hat{\mathbf{z}}\cdot\mathbf{H}_{\rm back}=\hat{\mathbf{z}}\cdot\mathbf{B}_{\rm back}/\mu_0$ is equal to the $\hat{\mathbf{z}}$ component of $\mathbf{H}$ everywhere due to the continuity of the tangential magnetic components; therefore, the integral of the $\hat{\mathbf{z}}$ component of the magnetic field $\mathbf{B}$ is proportional to the contrast of the relative magnetic permeability across the cross section of the cylindrical structure $\int_{(S)}(\mu_r-1)ds$ for an arbitrary inhomogeneous μ_r.

The Aharonov-Bohm measurements result in the value of flux $\int_{(S)}\mathbf{B}\cdot d\mathbf{s}$ or $\int_{(S)}\mathbf{B}_{\rm back}\cdot d\mathbf{s}$ depending on whether the cloaked object is present or not. The difference between these two quantities, which is equal to $\int_{(S)}\mathbf{B}_{\rm scat}\cdot d\mathbf{s}$, calculated by (2), indicates the possibility of AB detection of the cloaked object.

The relevant geometry of interest is shown in Fig. 1: the red arrows show the direction of the magnetic field, which cannot penetrate the 2D superconducting cylinder ($\rho<R_{\rm I}$, blue region). The properly selected cloak ($R_{\rm I}<\rho<R_{\rm II}$, light green region) deforms the path of the magnetic lines and the background field is restored all around the object. In this way, the scattered magnetic field in region III ($\rho>R_{\rm II}$,

white region) is identically zero. However, due to the presence of the axial ($\hat{\mathbf{z}}$) component of the background field $\mathbf{B}_{\text{back}}$ the magnetic flux through an open surface [defined by the closed boundary (C)] crossing the infinite cylinder is nonzero ($\oint_{(C)} \mathbf{A}_{\text{scat}} \cdot d\mathbf{l} \neq 0$), and thus the presence of the cloaked object is detectable in an Aharonov-Bohm experiment, by comparing two AB measurements with and without cloaked object.

B. Immunity to Aharonov-Bohm effect

Our goal now is to design an improved magnetostatic cloak that, while retaining a low scattering, does not affect Aharonov-Bohm measurements. In order to pursue such a goal, we need more degrees of freedom than just the two provided by the cloak permeability and thickness. For this reason, we split region II into U concentric layers, the uth of which occupies the shell $r_{u-1} < \rho < r_u$. The selection of the thickness of each 2D layer is not a crucial parameter and thus we make the assumption that each concentric cross section has the same area $(R_{\text{II}}^2 - R_{\text{I}}^2)/U$, namely

$$r_u = \sqrt{\frac{R_{\text{II}}^2 u + R_{\text{I}}^2 (U-u)}{U}}, \tag{3}$$

where $u = 1, \ldots, U$. The magnetic permeabilities μ_u are chosen to cancel the perturbation of the flux of $\mathbf{B}$ and restore a zero scattered potential. In order to avoid multiparametric nonlinear constraints whose global optimum is not easy to be determined, we consider permeabilities at each layer close to the optimal for scattering cancellation [11], namely we adopt the following perturbation form:

$$\mu_u = \mu_{\text{II}}(1 + s_u) = \frac{R_{\text{II}}^2 + R_{\text{I}}^2}{R_{\text{II}}^2 - R_{\text{I}}^2}(1 + s_u), \tag{4}$$

where $|s_u| \ll 1$ for $u = 1, \ldots, U$.

For technical reasons [21], we fix the permeability of the first and the last layer equal to the one of the 2D magnetostatic cloak (1), namely we take $s_1 = s_U = 0$. Under assumption (4), the zero contrast condition that secures immunity to the AB effect is written as

$$\sum_{u=2}^{U-1} s_u = -\frac{g^2 U}{g^2 + 1}, \tag{5}$$

where $g = R_{\text{I}}/R_{\text{II}}$ is the radii ratio. The condition (5) is obtained if we plug the expressions of the permeabilities from (4) into the equation $\sum_{u=1}^{U}(\mu_u - 1)(R_{\text{II}}^2 - R_{\text{I}}^2)/U + (\mu_1 - 1)R_{\text{I}}^2 = 0$. As far as the cloaking condition (zero scattering) is concerned, we follow the well-reported linearization procedure [21] of well-known objective functions of layered cylinders [22], obtaining the following constraint [valid only if $|s_u| \ll 1$ for $u = 2, \ldots, (U-1)$]:

$$\sum_{u=2}^{U-1} F_u s_u = 0, \tag{6}$$

where $F_u = \frac{(g^2-1)^2(u-1)u - g^2(g^2-1)(2u-1)U + 2g^4U^2}{[u+g^2(U-u)][(u-1)+g^2(U-u+1)]}$.

It should be stressed that a solution $\{s_2, \ldots, s_{U-1}\}$ which satisfies (5) has zero contrast, and thus the corresponding structure certainly exhibits full immunity to the Aharonov-Bohm effect. On the contrary, if a combination of perturbation parameters satisfies (6), it does not necessarily mean that their cylinders do not scatter the applied magnetostatic field, since the solution is a linear approximation of the far more complicated exact condition. However, we are considering a solution that is sufficiently close to the originally proposed (1) for cloaking. To be sure that we choose the solution $\{s_2, \ldots, s_{U-1}\}$ as close as possible to the magnetostatic cloak, $\mu_2 = \cdots = \mu_{U-1} = \mu_{\text{II}}$, and at the same time satisfy exactly (5) and (6), we require the minimization of the norm of the vector of the solution:

$$\text{Minimize} \sum_{u=2}^{U-2} s_u^2. \tag{7}$$

Conditions (5)–(7) formulate an analytically solvable optimization problem which yields

$$s_u = \frac{g^2 U}{g^2 + 1} \frac{\Sigma_2 - (U-2)\Sigma_1 F_u}{(U-2)\left(\Sigma_1^2 - \Sigma_2\right)}, \tag{8}$$

where $\Sigma_1 = \sum_{u=2}^{U-2} F_u$ and $\Sigma_2 = \sum_{u=2}^{U-2} F_u^2$.

The procedure is described in the inset of Fig. 2. We consider a map onto which we represent the device performance in terms of cloaking efficiency (how small the scattered magnetic field is) and in terms of immunity to the AB effect (how small the permeability contrast compared to vacuum is). Our goal is to get as close as possible to the origin of the plane. The proposed magnetostatic cloak corresponds to the purple point (ideal cloak but substantial permeability contrast). The linearization and optimization solution send

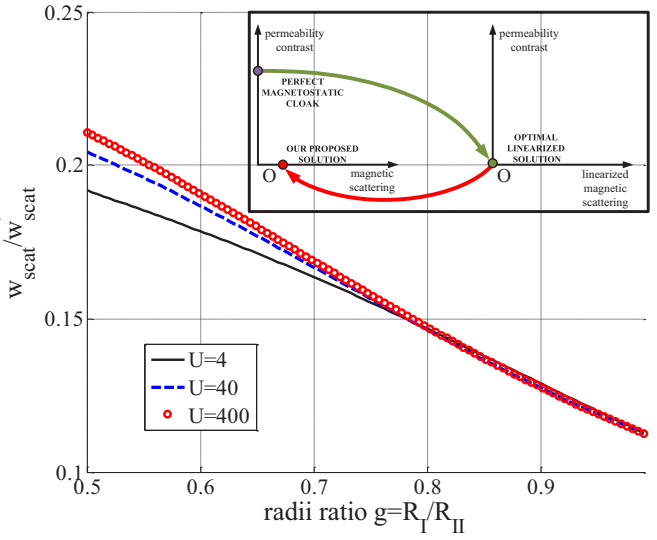

FIG. 2. (Color online) The ratio of the squared field produced by the cloaked object over the corresponding quantity in the uncloaked case $w_{\text{scat}}/w'_{\text{scat}}$ as a function of the radii ratio $g = R_{\text{I}}/R_{\text{II}}$ for several numbers of layers U. In the inset we show the description of the adopted design approach. We start from an ideal magnetostatic cloak with substantial contrast (purple point) and, by linearizing and solving the obtained optimization problem we move along the green arrow to the green point indicating ideal fulfillment of the design conditions (one of which is approximate). The same situation is represented by the red point, when the exact scattering is considered instead. We manage to make the structure with zero permeability contrast and relatively low scattering response.

us (via the green arrow) to the origin of the second map, whose horizontal axis is the linearized version of the scattered field (green point). In fact, the proposed object has nonzero scattering response, represented (via the red arrow) by the red point in the first map. In this way, we have converted a perfect cloak detectable by Aharonov-Bohm measurements to a structure totally immune to this effect, which still has a significantly reduced scattering response. Alternatively to the aforementioned procedure, one may employ other numerical optimization routines, implementing for instance genetic algorithms or a scanning along the domain of initial guesses. A fully optimized design goes beyond the scope of the present paper since our intention is to provide an analytical solution based on a physics inspired strategy with respect to the linearized objective function.

Recent papers have looked at solutions to neutralize the magnetic flux through certain regions of space in order to realize two-dimensional quantum cloaks, which may improve quantum experimental setups or bias measurements related to the paths of matter waves [23]. Similarly, transformation optics has been applied [24] on the quantum mechanics platform to design a cloak for quantum particles under AB effect. These studies ignore the classical electromagnetic aspects, and are not suitable for cloaking objects from magnetostatic or electromagnetic waves, while our proposed cloaks achieve magnetostatic cloaks that are also not detectable by quantum measurements.

Prior to concluding this section, we point out that the analysis presented here relies on the fact that the object under analysis is 2D and infinite. Interestingly, it is easy to realize that a 3D object of any size and shape, but of finite extent, would not be AB detectable if ideally cloaked. This is because the total flux of $\mathbf{B}$ through any closed surface is always zero ($\nabla \cdot \mathbf{B} = 0$). This implies that the flux of $\mathbf{B}_{\text{scat}}$ through any surface intersecting a 3D fully cloaked object has to be identically zero, because closing the surface around the object without further intersections would add zero to the flux of $\mathbf{B}_{\text{scat}}$. In the 2D scenario, on the contrary, one cannot close the intersecting surface without crossing again the object. In a realistic scenario, AB detectability refers to elongated objects (such as long cylinders), that are cloaked far from their edges, but that are not cloaked at the edge truncations. Far from the edges, and sufficiently close to the object, the scattered fields are consistent with the analysis presented here.

III. NUMERICAL RESULTS

A. Performance indicators

Without loss of generality (due to the cylindrical symmetry), we can assume that the background field does not possess an $\hat{\mathbf{x}}$ component. In the cylindrical coordinate system, the applied field is expressed as follows:

$$\mathbf{B}_{\text{back}} = \hat{\boldsymbol{\rho}} B_y \sin\varphi + \hat{\boldsymbol{\varphi}} B_y \cos\varphi + \hat{\mathbf{z}} B_z. \tag{9}$$

Due to the homogeneous nature of the excitation and the finite cross section of the scatterer, the form of the scattering component in region III is written in the form

$$\mathbf{B}_{\text{scat,III}} = \frac{M}{\rho^2}(-\hat{\boldsymbol{\rho}} \sin\varphi + \hat{\boldsymbol{\varphi}} \cos\varphi), \tag{10}$$

where M is a constant depending on the strength of the background field and the structure of the cylinder (measured in $\mathrm{T\,m^2}$). Since our design procedure achieves ideal undetectability by Aharonov-Bohm measurements, based on (6), we should measure the performance of the proposed device as a cloak. Two indicators are used: the first one gives us a metric of how much scattering is reduced by the presence of the cloak, defined as the ratio of the scattered energy density in the presence and in the absence of the cloak at any observation radius ρ (the result is independent from ρ):

$$\frac{w_{\text{scat}}}{w'_{\text{scat}}} = \frac{|\mathbf{B}_{\text{scat,III}}|^2}{|\mathbf{B}'_{\text{scat,III}}|^2} = \frac{M^2}{M'^2}. \tag{11}$$

The primed quantities correspond to (10) when only the superconducting core scatters the incoming illumination ($\mu_{\text{II}} = 1$). The second metric for our cloak is related to how much the spatial distribution of the overall field changes due to the (cloaked) scattering component. Therefore, we evaluate the ratio of scattered energy density of the cloaked object (along the worst-case surface $\rho = R_{\text{II}}$) over the energy density in the background field, namely

$$\frac{w_{\text{scat}}}{w_{\text{back}}} = \frac{|\mathbf{B}_{\text{scat,III}}|^2}{|\mathbf{B}_{\text{back}}|^2} = \frac{M^2 R_{\text{II}}^2}{B_y^2 + B_z^2}. \tag{12}$$

When we introduce an object with relative permeability μ_r inside region I, the complete immunity to the AB effect breaks down, since we modify the flux of $\mathbf{B}$ in the core, and thus a performance indicator comparing our design with the one of [11] should be defined. Since the phase shift experienced by the electrons in the Aharanov-Bohm effect depends on the magnetic flux concatenated with the path (C), we choose the ratio of the magnetic flux Φ_{scat} over the magnetic flux $\tilde{\Phi}_{\text{scat}}$ of the perfect cloak [11] as a measure of the detectability of the cloaked object using the Aharanov-Bohm effect. In particular, if we consider a two-dimensional cylindrical inclusion with cross-sectional area (S) and permeability μ_r inside the superconducting cylinder, this ratio is written as

$$\frac{\Phi_{\text{scat}}}{\tilde{\Phi}_{\text{scat}}} = \frac{S\mu_r}{S_I + S\mu_r}, \tag{13}$$

where $S_I = \pi R_{\text{I}}^2$ is the area of region I (superconducting material) and $S < S_{\text{I}}$. Obviously, the closer to the superconducting regime the inclusion material is ($\mu_r \to 0$) or the smaller is the size of that inclusion compared to the cloaked region ($S \ll S_{\text{I}}$), the scattering effect becomes weaker and weaker.

B. Results and discussion

In Fig. 2, we represent the ratio $w_{\text{scat}}/w'_{\text{scat}}$ defined in (11), as a function of the radii ratio $g = R_{\text{I}}/R_{\text{II}}$ varying the number of layers U. Surprisingly, our linearized solution yields better performance for thinner cloaks. In particular, for $g > 0.8$ the result is the same regardless of the number of segments U. The scattered power is reduced by over 85% in such thin cloaks, which constitutes a quite efficient design. For thick cloaks the performance deteriorates in the case of more layers U, despite the fact that more free parameters are simultaneously varying. Such an unexpected result is attributed to the fact that the linearization of the cloaking condition is less

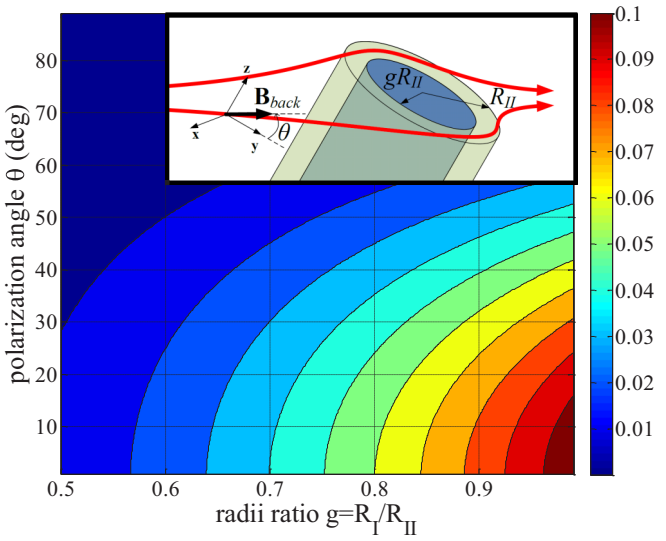

FIG. 3. (Color online) The ratio of the squared fields produced by the cloaked object over the squared magnitude of the (homogeneous) background field $w_{\rm scat}/w_{\rm back}$ in contour plot with respect to the radii ratio $g = R_{\rm I}/R_{\rm II}$ and the polarization angle θ. The definitions of g and θ are shown in the embedded figure.

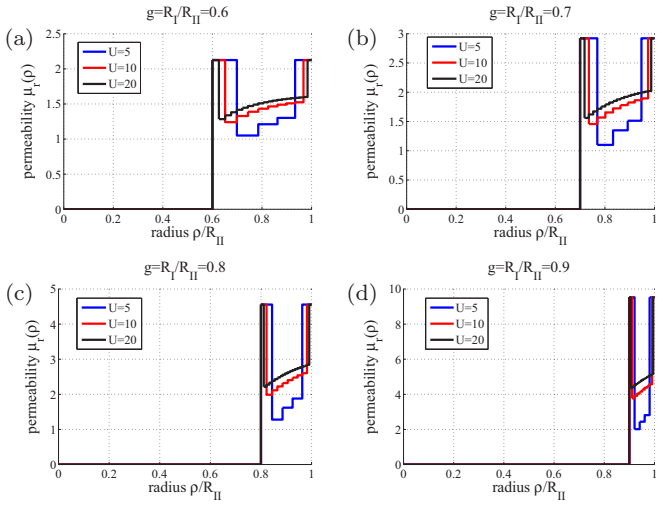

FIG. 4. (Color online) Optimal permeability profiles $\mu_r(\rho)$ with respect to the normalized radius $\rho/R_{\rm I}$ for several discretization numbers U with (a) $g = R_{\rm I}/R_{\rm II} = 0.6$, (b) $g = R_{\rm I}/R_{\rm II} = 0.7$, (c) $g = R_{\rm I}/R_{\rm II} = 0.8$, and (d) $g = R_{\rm I}/R_{\rm II} = 0.9$.

successful for larger U; accordingly, the difference between the actual scattering response and its linearized version gets more significant.

In Fig. 3, we show the ratio $w_{\rm scat}/w_{\rm back}$ defined in (12), in contour plot with respect to the radii ratio $g = R_{\rm I}/R_{\rm II}$ and the polarization angle θ of the homogeneous background magnetic field $\mathbf{B}_{\rm back} = B_0(\hat{\mathbf{y}}\cos\theta + \hat{\mathbf{z}}\sin\theta)$. Obviously, the scattering decreases for larger polarization angles θ since the axial magnetostatic field does not respond to a permeability contrast. On the other hand, for thinner cloaks the perturbation of the background field is larger, although it always remains limited below 10%. Accordingly, the cloaked object does not substantially modify the background field distribution.

In Fig. 4, we show the distributions of the magnetic permeability for $0 < \rho < R_{\rm II}$ for various numbers of segments U of the clad and several radii ratios $g = R_{\rm I}/R_{\rm II}$. We notice that the required permeabilities are larger for thinner cloaks, as expected. Furthermore, the optimal permeabilities differ less from the value $\mu_{\rm II}$, when more layers U are considered, a conclusion which could be anticipated since more degrees of freedom are available and thus a solution with smaller perturbations from the standard permeability is achievable. It should be noted that the layers are magnetically denser in the inside layers than the outside, regardless of the choice of the other parameters. The considered permeability values in the examples presented here are quite reasonable, and close to values available in natural materials. The optimization may be adjusted by adding constraints on the permeability of available materials, at the cost of adding more layers.

IV. CONCLUSIONS

Magnetostatic cloaks constitute an interesting class of cloaking devices, with relevant technological applications, and with implications that govern also the cloak response at higher frequencies. However, even if one can achieve perfect magnetostatic cloaking, we have shown here that a 2D object may still be noninvasively detected from the outside by measuring the modification of magnetic flux, regardless of its physical size, exploiting Aharonov-Bohm measurements. Here we have devised new designs that allow an optimal multilayered cladding, with which the scattered magnetic flux vanishes, and simultaneously the scattering response of the entire system gets substantially suppressed. Such an approach can pave the way to the design of equipment providing extremely low detectability from both to magnetostatic and quantum measurements. We stress again, as done in the main body, that AB detectability does not hold for a fully cloaked 3D object, but it applies to elongated objects that are not ideally cloaked at their edges, a case of relevance in conventional AB setups.

ACKNOWLEDGMENTS

A.A. would like to acknowledge stimulating discussions with Professor A. Sanchez and his group at the Universidad Autonoma de Barcelona, Spain. This work was supported by the National Science Foundation with Grant No. ECCS-0953311 and by the Air Force Office of Scientific Research with Grant No. FA9550-13-1-0204.

[1] J. B. Pendry, D. Schurig, and D. R. Smith, Controlling electromagnetic fields, Science **312**, 1780 (2006).

[2] A. Alù and N. Engheta, Achieving transparency with plasmonic and metamaterial coatings, Phys. Rev. E **72**, 016623(2005).

[3] A. Alù, Mantle cloak: Invisibility induced by a surface, Phys. Rev. B **80**, 245115 (2009).
[4] F. Monticone and A. Alù, Do Cloaked Objects Really Scatter Less? Phys. Rev. X **3**, 041005 (2013).
[5] E. M. Purcell, On the absorption and emission of light by interstellar grains, Astrophys. J. **158**, 433 (1969).
[6] M. Gustafsson, C. Sohl, and G. Kristensson, Physical limitations on antennas of arbitrary shape, Proc. R. Soc. A **463**, 2589 (2007).
[7] F. Monticone and A. Alù, Physical bounds on electromagnetic invisibility and the potential of superconducting cloaks, Phot. Nano. Fund. Appl. **12**, 330 (2014).
[8] B. Wood and J. B. Pendry, Metamaterials at zero frequency, J. Phys.: Condens. Matter **19**, 076208 (2007).
[9] F. Magnus, B. Wood, J. Moore, K. Morrison, G. Perkins, J. Fyson, M. C. K. Wiltshire, D. Caplin, L. F. Cohen, and J. B. Pendry, A d.c. magnetic metamaterial, Nat. Mater. **7**, 295 (2008).
[10] A. Sanchez, C. Navau, J. Prat-Camps, and D.-X. Chen, Antimagnets: controlling magnetic fields with superconductor-metamaterial hybrids, New J. Phys. **13**, 093034 (2011).
[11] F. Gömöry, M. Solovyov, J. Souc, C. Navau, J. Prat-Camps, and A. Sanchez, Experimental realization of a magnetic cloak, Science **335**, 1466 (2012).
[12] J. Souc, M. Solovyov, F. Gömöry, J. Prat-Camps, C. Navau, and A. Sanchez, A quasistatic magnetic cloak, New J. Phys. **15**, 053019 (2013).
[13] R. Wang, Z. Lei Mei, and T. J. Cui, A carpet cloak for static magnetic field, Appl. Phys. Lett. **102**, 213501 (2013).
[14] Y. Ahanorov and D. Bohm, Significance of electromagnetic potentials in the quantum theory, Phys. Rev. **115**, 485 (1959).
[15] A. Tonomura, N. Osakabe, T. Matsuda, T. Kawasaki, J. Endo, S. Yano, and H. Yamada, Evidence for Aharonov-Bohm Effect with Magnetic Field Completely Shielded from Electron Wave, Phys. Rev. Lett. **56**, 792 (1986).
[16] M. D. Semon and J. R. Taylor, The Aharonov-Bohm effect: Still a thought-provoking experiment, Found. Phys. **18**, 731 (1988).
[17] H. Batelaan and A. Tonomura, The Aharonov-Bohm effects: Variations on a subtle theme, Phys. Today **62**(9), 38 (2009).
[18] M. Bayer, M. Korkusinski, P. Hawrylak, T. Gutbrod, M. Michel, and A. Forchel, Optical Detection of the Aharonov-Bohm Effect on a Charged Particle in a Nanoscale Quantum Ring, Phys. Rev. Lett. **90**, 186801 (2003).
[19] M. J. Arman and C. Chase, Aharonov-Bohm sensor, United States Patent No. 0032730, 2013.
[20] H. Peng, K. Lai, D. Kong, S. Meister, Y. Chen, X.-L. Qi, S.-C. Zhang, Z.-X. Shen, and Y. Cui, Aharonov-Bohm interference in topological insulator nanoribbons, Nat. Mater. **9**, 225 (2010).
[21] C. A. Valagiannopoulos and N. L. Tsitsas, Linearization of the T-matrix solution for quasi-homogeneous scatterers, J. Opt. Soc. Am. **26**, 870 (2009).
[22] C. A. Valagiannopoulos, Semi-analytic solution to a cylindrical microstrip with inhomogeneous substrate, Electromagnetics **27**, 527 (2007).
[23] D.-H. Lin and P.-G. Luan, Cloaking of matter waves under the global Aharonov-Bohm effect, Phys. Rev. A **79**, 051605 (2009).
[24] D.-H. Lin, Transformation design method for quantum states, Phys. Rev. A **85**, 053605 (2012).